In Situ Photochemical Transformation of Hg Species and Associated Isotopic Fractionation in the Water Column of High-Altitude Lakes from the Bolivian Altiplano

Sylvain Bouchet, Emmanuel Tessier, Jeremy Masbou, David Point, Xavier Lazzaro, Mathilde Monperrus, Stéphane Guédron, Dario Acha, David Amouroux

In Situ Photochemical Transformation of Hg Species and Associated Isotopic Fractionation in the Water Column of High-Altitude Lakes from the Bolivian Altiplano

Sylvain Bouchet, Emmanuel Tessier, Jeremy Masbou, David Point, Xavier Lazzaro, Mathilde Monperrus, Stéphane Guédron, Dario Acha, David Amouroux

In situ Hg species photochemical transformations and associated isotopic fractionation in the water column of high-altitude lakes from the Bolivian Altiplano

S. Bouchet[1†*], E. Tessier[1], J. Masbou[2], D. Point[2,3], X. Lazzaro[3,4], M. Monperrus[1], S. Guédron[5,6], D. Acha[3], D. Amouroux[1],

[1] Universite de Pau et des Pays de l'Adour, E2S/UPPA, CNRS, Institut des sciences analytiques et de physico-chimie pour l'environnement et les matériaux (IPREM), 64000, Pau, France

[2] Géosciences Environnement Toulouse (GET), Univ. Paul Sabatier, CNRS, IRD, Observatoire Midi Pyrénées (OMP), 14 avenue Edouard Belin, 31400 Toulouse, France

[3] Unidad de Calidad Ambiental (UCA) – Instituto de Ecologia - Universidad Mayor de San Andres, Campus Universitario de Cota Cota, Calle 27, La Paz, Bolivia.

[4] Unité Biologie des Organismes et Ecosystèmes Aquatiques (BOREA), Muséum National d'Histoire Naturelle, Sorbonne Université, Université Caen-Normandie, Université des Antilles, CNRS, IRD. 61 rue Buffon, 75231 Paris CEDEX 5, France

[5] Univ. Grenoble Alpes, Univ. Savoie Mont Blanc, CNRS, IRD, IFSTTAR, ISTerre, 38000 Grenoble, France.

[6] Laboratorio de Hidroquímica - Instituto de Investigaciones Químicas - Universidad Mayor de San Andrés, Campus Universitario de Cota-Cota, casilla 3161, La Paz, Bolivia.

[†]Present address: ETH Zürich, D-USYS department, Universitätstrasse 16, CH-8092 Zürich, Switzerland

*Corresponding author: sylvain.bouchet@usys.ethz.ch; +41 58 765 5461

ABSTRACT

Photochemical reactions are major pathways for the removal of Hg species from aquatic ecosystems, lowering the concentration of monomethylmercury (MMHg) and its bioaccumulation in foodwebs. Here we investigate the rates and environmental drivers of MMHg photodegradation and inorganic Hg (IHg) photoreduction in waters of two high altitude lakes from the Bolivian Altiplano representing meso- to eutrophic conditions. We incubated three contrasting waters *in-situ* at two depths after adding Hg enriched isotopic species to derive rate constants. We found that transformations mostly occurred in subsurface waters exposed to UV radiations and were mainly modulated by the dissolved organic matter (DOM) level. In parallel, we incubated the same waters after the addition of low concentrations of natural MMHg and followed the stable isotope composition of the remaining Hg species by compound-specific isotope analysis allowing the determination of enrichment factors and MIF signatures during *in-situ* MMHg photodegradation in natural waters. We obtained similar enrichment factors for the three waters (average $\varepsilon_{\delta 202}$ = -7.1 ± 0.9 ‰ and $\varepsilon_{\Delta 199}$ = -4.8 ± 0.3 ‰, 1 SE) but the expression of the mass independent fractionation ($\Delta^{199}Hg/\Delta^{201}Hg$ ratio) diverged depending on the DOM level. The $\Delta^{199}Hg/\Delta^{201}Hg$ ratios ranged from 1.24 ± 0.03 to 1.34 ± 0.02 for the low and high DOM waters, respectively and matched very well the signatures of MMHg recorded in fish (Orestia spp) collected in the same lake. The average extent of MMHg photodegradation before its incorporation into the foodwebs from each lake ranged from 10 % in the eutrophic waters to 26 % in the mesotrophic ones, which explain the higher Hg concentrations in biota observed in the eutrophic lake. Our results call for more photodegradation experiments to be conducted under natural conditions in order to accurately use Hg isotopes signatures recorded in biota to determine the extent of Hg species transformations and lifetime in aquatic ecosystems.

Keywords: photodegradation; photoreduction; compound specific isotope analysis; enrichment factor; dissolved organic matter; fish

Synopsis: MMHg photodegradation in lake waters was found to be modulated by DOM whereas the associated Hg isotopes fractionation matched the Hg signatures recorded in fish.

INTRODUCTION

Hg concentrations have increased in all environmental compartments since the industrial revolution due to massive release from anthropogenic activities.[1] In aquatic ecosystems, a fraction of the inorganic Hg (IHg) is transformed to monomethylmercury (MMHg), which is the form that biomagnifies in food webs leading to human exposure.[2,3] IHg methylation is mostly carried out by bacterial strains possessing a specific genes cluster[4] that is found in nearly all anaerobic environments.[5] Depending on the ecosystem, the major contributors to the MMHg pool include i) water saturated systems (e.g., flooded soils and sediments)[6], ii) the suboxic part of water column,[7,8] and iii) anoxic microniches found in oxic waters such as particulate flocs and biofilms.[9,10] However, the Hg pools available to aquatic organisms for subsequent methylation or trophic transfer result from the balance between multiple reactions. Among these, IHg reduction and MMHg demethylation are considered important pathways reducing the pool of IHg available for its methylation into MMHg and its further biomagnification.

In the aphotic zone, reduction and demethylation can be performed by various microorganisms carrying dedicated genes or not.[11–14] The abiotic reduction of IHg at the surface of Fe(II)-bearing minerals is also well established as a significant pathway[15,16] while its reduction by OM[17] is less certain, depending on the OM redox state, concentration and composition.[18,19] In the euphotic zone, photochemically induced reactions are considered a major sink of IHg and MMHg in natural waters.[20,21] These reactions are likely proceeding through multiple pathways depending on the environmental conditions[22] and several controlling parameters have been identified, among which light and dissolved organic matter (DOM) are especially important. Regarding light, both the radiation intensity[20,21,23] and wavelength are influential, with the shortest wavelengths (i.e. UVB: 280 - 320 nm) being the most effective at triggering the reactions.[21,24,25] UV radiations therefore contribute the most to MMHg degradation and IHg reduction near the surface but they are rapidly attenuated with depth and the photosynthetic active radiation (PAR) could therefore be responsible for the largest share of the transformations over the whole water column.[22]

On the other hand, DOM concentration and composition influence both reactions, e.g. by controlling the light transmission, production/consumption of reactive oxygen species (ROS) and Hg complexation.[26–29] Photochemical reactions typically proceed more efficiently in the presence of DOM but reaction rates usually decrease at high DOM concentrations.[30,31] The breaking point depends on the DOM properties driving light attenuation and quenching of radical species.[27,32] While the direct photoreduction of IHg bound to DOM is possible under natural light conditions,[33] the direct photolysis of MMHg is not,[31] and MMHg complexation by thiol groups is a key

determinant of its photodegradation as it weakens the Hg-C bond.[31,34] Laboratory studies further showed that the reaction proceeds faster when MMHg is bound to the thiol group of a molecule also containing an aromatic moiety.[35,36] It suggests an intramolecular mechanism resulting from the direct energy transfer between the excited triplet state of DOM (^{3}DOM*) and the Hg-C bond, while indirect mechanisms involving several ROS were previously suggested from field experiments.[22]

Before entering the food-chain as MMHg, Hg species undergo a series of biogeochemical pathways affecting their stable isotope composition, with both mass-dependent (MDF) and mass-independent fractionations (MIF) being observed.[37] For instance, positive or negative MDF is observed for all kind of biotic and abiotic pathways, whereas MIF of odd Hg isotopes is specifically observed for photochemical processes occurring in surface waters due to the magnetic isotope effect (MIE).[38] Since its first demonstration in 2007,[39] several studies have examined Hg-MIF during MMHg photodegradation and IHg photoreduction in synthetic waters of various composition but never in natural waters due to analytical constraints. The MIF direction and signature (Δ^{199}Hg/Δ^{201}Hg) have been shown to vary depending on both the reaction involved, the light wavelength and the Hg bonding environment.[40–44] MIF enrichment factors determined in synthetic waters have been used to derive useful conclusions on Hg cycling in aquatic ecosystems such as the extent of MMHg photodegradation before its uptake by biota. A paradox however remains in that the MIF signatures observed in these laboratory experiments do not accurately match the one recorded in biota.[43]

In previous studies, we have examined several aspects of Hg cycling in lakes of the Bolivian Altiplano (3600-3800 m a.s.l.) which are highly reactive ecosystems where methylation can be stimulated under eutrophicated conditions.[45] We provided a Hg contamination level and speciation inventory[46] and especially studied the Hg accumulation and transformations in sediments, periphyton and benthic biofilms.[47–50] We pointed out to sediments and biofilms as compartments of MMHg production and bioaccumulation, but pathways leading to MMHg and Hg removal were not addressed so far. Here, we specifically investigated Hg species transformations in the water column of the same lakes, with a focus on demethylation and reduction as well as related isotope fractionation, to get more insights into the fate of Hg before its incorporation in foodwebs. We carried out *in situ* incubation experiments at two depths (with and without UV) using lake water from several sites showing contrasted DOC levels and the addition of isotopically enriched tracers to determine transformations rate constants. In parallel experiments, addition of low concentrations of natural MMHg allowed to determine the enrichment factors and MIF

104 signature during the photodegradation of MMHg in these waters. This information was then compared to the MMHg
105 isotopic composition recorded in fish from each lake to estimate the extent of MMHg photodegradation in their water
106 column and discuss the control exerted by DOM.

2. EXPERIMENTAL SECTION

2.1. Study sites.

Lake Titicaca (3809 m a.s.l.) comprises two connected basins, the Great Lake (7,131 km²; mean depth = 100 m) and the Small Lake (1,428 km²; mean depth = 9 m). Each basin is fed by multiple streams that bring in various pollutants according to their watershed characteristics (urban, industrial, mining or agricultural activities).[46] Lake Uru Uru (3686 m a.s.l., 120 to 350 km^2 and 0.25 to 1 m depth) is a human-made reservoir located in the central part of the Bolivian Altiplano, where numerous mining and smelting activities are concentrated. Sampling stations were selected to represent various biogeochemical conditions of the hydrosystem in term of temperature, pH, conductivity, dissolved oxygen, redox and DOC concentrations (Figure SI-1 and Table SI-1): CH is an oligotrophic deep station (38 m) whereas HU presents an intermediate depths (5 m) and mesotrophic conditions. BC and UU are both shallow (0.25 – 2 m) eutrophicated stations receiving mixed urban and mining effluents. A preliminary campaign was conducted in November 2013 and two main campaigns were carried out in 2014, the first by the end of the rainy season (April-May) and the second by the end of the dry one (October-November). Meteorological data were recorded by a weather station (Campbell Scientific, Logan, UT, USA; equipped with a CR1000 datalogger) installed on the shore of the Small Lake near the incubation sites whereas the spectral attenuation of light (UV-PAR) through the water column was monitored with an underwater profiling C-OPS spectroradiometer (Biospherical instrument Inc., San Diego, CA, USA).[51]

2.2. Sampling and incubations.

Lake water samples were collected at each station a few hours before incubations using a trace-metal clean 5-L Teflon-lined General Oceanic (GO-FLO) bottle. Water was distributed in 125- or 250-mL Teflon® (Nalgene PFA) bottles for incubations with enriched isotopic tracers or natural MMHg (Strem chemicals), respectively (Fig SI-2). On one hand, Hg species transformations rate constants were determined using isotopically enriched tracers added within ambient concentration ranges (0.1 to 0.2 $ng.L^{-1}$ for $^{201}MMHg$ and 0.8 to 1.6 $ng.L^{-1}$ for ^{199}IHg). Three controls (t_0) per series were immediately acidified and stored in the dark at +4 °C, with half of the other bottles being mounted on a homemade system (Figure SI-2) and incubated *in situ*. Incubations of samples from CH, HU and BC were all conducted at the HU station with samples from HU and CH incubated at two different depths (0.5 and 3.5 m) to discriminate the importance of specific light wavelengths. The remaining bottles were incubated in the dark in lake

surface water. Every incubation series were carried out in triplicates for the same period (4 to 8 hours) and eventually stopped by acidification before being stored at +4 °C in the dark. On the other hand, Hg stable isotope fractionation patterns during MMHg degradation were investigated by spiking lake water with natural MMHg (200 ng.L^{-1}) and a similar strategy as above but with longer incubations and a sacrificial sampling strategy where 3 bottles were sampled at 6, 12, 24 and 36 hours. One dark control incubation was also carried out for each site but sampled only at 36 h, corresponding to the final time point of the diurnal incubation.

Fish samples analyzed in this study consist of muscles from several individuals of Orestias Spp (n_{total} = 43), an endemic fish species of the Bolivian Altiplano region.[52] Most of them were collected by local fishermen using gillnets during dedicated scientific surveys performed in Lake Titicaca (n=15) and lake Uru Uru (n=28) in October 2010 (9 additional samples from 2005 and 2014 were added to the database) and were preserved at – 20°C before being freeze-dried and homogenized. MMHg compound specific stable isotope analysis (CSIA) was carried out for all fish samples using the methodology detailed previously.[53]

2.3. Laboratory analyses.

Ancillary data.

Dissolved organic carbon (DOC) concentrations were determined using a Non Dispersive Infra-Red (NDIR) CO_2 Shimadzu® (Model VCSN) spectrometer after wet oxidation in a sodium persulfate solution at 100 °C. Specific ultraviolet absorbance at 254 nm ($SUVA_{254}$) was obtained by dividing the UV absorbance measured with an UV-VIS (Perkin Elmer Lambda 35) by the DOC concentration of the same water sample. A submersible multiparameter probe (HANNA HI-9828, Hanna Instruments) was used to characterize the basic physicochemical conditions (pH, conductivity, dissolved oxygen concentration, oxygen saturation, and temperature).

Hg species concentrations and calculation of transformation rates.

Directly after incubations, Hg^0 was purged from the samples onto gold-coated sand traps and analyzed according to protocols previously described.[54] Teflon® purging vessels (0.5 L) were bubbled for 30 min with a Hg-free nitrogen flow (c.a. 400 mL min^{-1}) and the gas stream was dried through a moisture trap before species trapping. Gold traps were analyzed on-site (within a few hours) by double amalgamation on gold (method detection limit about 2 fM). IHg and MMHg concentrations were determined back in the laboratory according to Rodriguez-Gonzalez et al.[55]

Briefly, Hg species were analyzed by species-specific isotope dilution using a complementary pair of isotopes (^{198}IHg and ^{202}MMHg), derivatization with sodium tetrapropylborate and liquid-liquid extraction into isooctane. After a vigorous shake, the organic phase was recovered and injected in triplicate into the gas chromatograph (GC) hyphenated to an inductively coupled plasma mass spectrometer (ICP-MS, Thermo-Electron Series XII). The concentrations of the added and formed Hg species deriving from the enriched isotopes 199 and 201 were calculated by isotopic pattern deconvolution methodology and the demethylation rate was calculated based on the loss of ^{201}MMHg. The determination of IHg and MMHg concentrations in the incubations with added natural MMHg was carried out according to Monperrus et al.,[56] using ^{199}IHg and ^{201}MMHg, on a small subsample (1.5 mL).

Hg compounds specific stable isotope analysis (CSIA) for water samples.

IHg and MMHg CSIA were determined by on-line preconcentration, separation by gas chromatography and detection by MC-ICP-MS as described in details in Bouchet et al.[57] Briefly, 100 mL of the incubated water were derivatized with sodium tetrapropylborate and extracted into hexane, of which 25 µL were injected into the GC using a programmed temperature vaporization injector. A straight liner (2 mm ID, 2.75 mm OD, 120 mm length, ThermoFisher Scientific, France) packed with a styrene-divinylbenzene polymeric resin (Bondesil-ENV, 125 µm, Agilent Technologies) was used to preconcentrate the Hg species on-line before their separation and detection by GC/MC-ICP-MS. A Trace Ultra GC (ThermoFisher Scientific, France) was fitted with a MXT-1 capillary column (0.53 mm ID, 1 µm thick coating, 30 m length, Restek, France) and interfaced to a Nu Plasma HR (Nu instruments, UK) through a commercial heated interface and dual inlet glass torch allowing the simultaneous introduction of an isotopically certified Tl solution (200 µg.L^{-1} in 2% HNO_3) to correct for instrumental mass bias. Analysis followed a Sample Standard Bracketing (SSB) sequence were the SRM NIST SRM-3133 (IHg) and STREM (MMHg) were used as primary standards and matched to the sample concentrations within 25%. Isotopic ratios were calculated using the Linear Regression Slope (LRS) method and Hg isotopic compositions are commonly reported as delta values relative to the NIST SRM-3133 IHg standard.[58] For IHg, delta values were calculated as follow:

$$\delta^{xxx}IHg(‰) = \left[\frac{(^{xxx}Hg/^{198}Hg)_{sample}}{(^{xxx}Hg/^{198}Hg)_{NIST\ 3133}} - 1\right] \times 1000$$

Where xxx can be 204, 202, 201, 200 or 199 and $(^{xxx}Hg/^{198}Hg)_{NIST\ 3133}$ is the averaged isotopic ratio of the two bracketing standards. For MMHg, the delta values were first calculated against the STREM MMHg standard and then converted relatively to the NIST SRM-3133 according to:

$$\delta^{xxx}MMHg(‰) = \left[\left(\frac{\delta^{xxx}(STREMvsNIST3133)_{CCVG}}{1000}+1\right)\times\left(\frac{\delta^{xxx}(samplevsSTREM)}{1000}+1\right)-1\right]\times 1000$$

where δ^{xxx} (STREM vs NIST SRM-3133)$_{CCVG}$ is the previously reported isotopic composition of the STREM MMHg standard relative to the NIST SRM-3133 measured by CCVG / MC-ICP-MS[59] and δ^{xxx} (sample vs STREM) is the isotopic composition of the sample MMHg versus the STREM MMHg standard calculated as follows:

$$\delta^{xxx}SamplevsSTREM(‰) = \left[\frac{(^{xxx}Hg/^{198}Hg)_{sample}}{(^{xxx}Hg/^{198}Hg)_{STREM}}-1\right]\times 1000$$

The Δ notation is used to express the mass independent fractionation (MIF), calculated as $\Delta^{xxx}Hg = \delta^{xxx}Hg - \beta_{kin}\times\delta^{202}Hg$ where $\beta_{kin} = \ln(m_{198}/m_{xxx})/\ln(m_{198}/m_{202})$.[58] Enrichment factors were calculated as the slope of the best linear fit of relation between $\ln(\Delta^{199}Hg)$ or $\ln(\delta^{202}Hg)$ and ln(f).

RESULTS AND DISCUSSION

Characteristics of the water column at the investigated stations.

Both lakes are influenced by a high-altitude tropical climate (rainy season between December and March) and their hydrological regime is dominated by evaporation. This results in high pH values (Table SI-1), usually ranging from 7.4 to 9.5 although lower values are found at the BC station (6.6 – 7.1) due to severe anthropogenic inputs and OM mineralization.[60] Conductivity (~ 1100 - 6200 µS.cm^{-1}) and DOC concentrations (2.5 - 29 mg L^{-1}) overall reflect the eutrophication status of each station with a gradual increase from CH to UU while the oxygen saturation (15 – 183 %) shows an inverse trend. SUVA values in Lake Titicaca increase with the DOC values but remain overall low (0.004 – 0.07 L mg^{-1} m^{-1}) due to limited terrestrial inputs from the watershed and thus the prevalence of autochthonous OM in the lake. Typical incident PAR intensities along the day and specific wavelength penetration depths in the water column are presented in Figure SI-3. The daily and seasonal variations of light attenuation were limited (< 10 %, data not shown). At the CH and HU station where incubations were carried out and representative for lake water DOC concentrations of 2 – 3 mg L^{-1}, PAR radiations could reach down to about 8 m while UV-A are attenuated between 3 and 8 m depending on the wavelength and UV-B are not transmitted at all below 3m.

Hg species transformations in the water column.

For the various conditions investigated, the demethylation rate constants stretched over an order of magnitude but were relatively constant for each station independent of the season (Figure 1) and fell in two groups, which clearly differ in their DOC concentrations. The demethylation at CH and HU (0.003 – 0.018 h^{-1}, DOC 2.6 – 4.5 mg L^{-1}) were indeed consistently lower than at BC and UU (0.036 – 0.05 h^{-1}) where the DOC concentration is usually 2 – 3 times higher (6.1 – 9.9 mg L^{-1}, Table S1). The demethylation rates were on average 25 % lower in bulk than in filtered waters exposed to light. It implies that the photodegradation reaction is mainly induced by DOM and that the presence of particles (including bacteria and algae) hamper it through both attenuated light transmission (absorption & scattering) and radical scavenging. The demethylation rates largely decreased (3 to 8 times) for the incubations conducted at depth (3.5 m) compared to the subsurface ones (0.5 m) reflecting the sharp attenuation of (UV) light and especially UV-B with depth (Figure SI-3). In the dark controls, rates were always below (or very close) to detection limits (DLs). The relationship between MMHg photodegradation and DOC concentration follows a bell curve with a maximum around 6 mg L^{-1} (Figure SI-4). This is consistent with previous studies demonstrating that a

minimal amount of DOM is required to complex MMHg and trigger the photodegradation process[31,34,61] but that photodegradation rates decrease with an increase in DOM due to light attenuation and radical scavenging.[32,62,63] Interestingly, Girard et al.[64] found a very similar relationship in Arctic lakes spanning DOC contents from about 1 to 11 mg L^{-1}, with a breaking point around 7 mg L^{-1}.

Similarly to MMHg demethylation, the IHg reduction rates were also relatively constant within the stations and independent of the season. They fell in the same two groups (Figure 1) but exhibited an opposite trend with respect to demethylation, i.e. higher at CH and HU (0.009 – 0.017 h^{-1}) than at BC and UU (0.003 – 0.004 h^{-1}). There is overall a negative trend with DOC (Figure SI-4) suggesting that the optimal DOC concentration for IHg reduction lies in the lower range examined here (< 5 mg L^{-1}) and higher concentrations only decrease the reaction rate. The reduction rates dropped by 2 to 7 times for the incubations conducted at depth (CH and HU) compared to the subsurface samples, reflecting again the UV attenuation. The reduction rates in the dark were negligible (< 0.001 h^{-1}) demonstrating that the dark biotic or abiotic contribution to reduction was limited within the experiment timeframe, except for HU during the dry season (0.002 – 0.003 h^{-1}).

No methylation was detected in waters during the two seasons investigated. However, our incubations were all carried out during daytime while most methylating bacteria are (facultative) anaerobic and could thus be more active at night when the oxygen level decreases. Moreover, the high ambient MMHg concentrations, especially in BC and UU (73 – 1030 pg L^{-1}, Table SI-1), make it difficult to detect the formation of new MMHg from the low concentrations of added IHg (1 - 1.5 ng L^{-1}). Therefore, methylation in the water columns of these lakes cannot be ruled out from these experiments with enriched tracers. Methylation was however detected in waters from UU incubated with stable isotopes during the dry season (see below), consistent with previous observations in this shallow lake where strong redox shift and high concentrations of suspended particles favor the establishment of reducing microniches and restrict photodemethylation in the water column.[47,65] Regarding Lake Titicaca, several compartments can contribute to the pool of MMHg present in the water column as methylation was previously clearly demonstrated in benthic biofilms, green-algae periphyton and carbonate-rich sediments[49,50] but also in the water column itself under anoxic conditions that developed after a severe algal bloom.[45]

MMHg photodegradation and associated isotopic fractionation in the water column.

Hg species concentrations along incubation experiments.

No significant loss of MMHg (or increase in IHg) was observed in the dark controls incubated for 36 h in the dark for each site or in the incubation performed with HU water at 3.5 m depth, where mostly PAR with little UV-A (< 10% of the incident surface radiation) but no UV-B radiations are transmitted (Figure SI-3). The results of these experiments conducted over a longer duration and with higher MMHg concentrations compared to the incubations with enriched isotopes (200 vs 0.2 ng.L^{-1}) confirmed that demethylation in the dark or at 3.5 m, below the UV-B penetration depth, was not significant. In the three sets of incubations carried out at 0.5 m, the MMHg concentrations decreased from an initial value close to 200 ng L^{-1} to a final value ranging from 140 to 170 ng L^{-1} (Figure 2). A first decrease was observed between 0 and 6 h for all but then the time-courses diverged during the night period (10 – 22 h): the MMHg concentrations were either still decreasing (BC, high demethylation rate), stable in HU (moderate demethylation rate) or slightly increasing in UU, which indicates a re-methylation of the produced IHg. A decrease was finally observed for all incubations during the second day (24 - 36 h). At 6h, the average demethylation rate constants obtained from triplicate experiments were thus 0.011 ± 0.003, 0.036 ± 0.006 and 0.036 ± 0.002 h^{-1} for HU, BC and UU, respectively. These values are consistent with those previously obtained from the enriched isotope incubations, i.e. 0.010, 0.030 and 0.046 for HU, UU and BC, respectively (see above). It demonstrates a similar behavior for the photodegradation of the added MMHg, despite the concentrations being more than 1000 times higher, extending previous observations made on added versus ambient MMHg.[25]

On the other hand, the concentrations of IHg increased from 6 ± 2, 9 ± 3 and 10 ± 1 ng L^{-1} in BC, UU and HU respectively to 30 ± 5, 21 ± 1 and 23 ± 5 ng L^{-1} after 36 h (Figure 2). The IHg concentrations showed the inverse trend relative to the MMHg losses, i.e. a first increase followed by a plateau during the night period and a second increase during the next day. On average, only 30 % of the lost MMHg was recovered as IHg in the solution at the end of the experiment (Figure SI-6) but the recovery was higher for HU and BC than UU (45, 37 and 20 %, respectively at 36 h). These losses cannot be solely explained by the production and evasion of Hg° as the reduction rates are lower than the demethylation ones and exhibit an inverse trend (HU >> UU ≥ BC). Altogether, this suggests that the missing IHg fraction also comprises a refractory phase that escapes the derivatization (propylation) reaction needed prior to GC-ICP-MS analysis. We hypothesize that IHg was gradually transformed into HgS nanoparticles along the incubations, most likely by direct precipitation with sulfides produced through sulfate reduction occurring in low oxygen microniches.[47] However, HgS was also observed to form within a few hours upon UV exposure of IHg complexed with thioglycolic acid[66] and in the dark when IHg is left aging with OM

for a long period.[67] The occurrence of sulfate reduction in microniches of UU waters is very plausible given: (i) the high DOM, SPM and sulfate that favor the development of aggregates,[47] and (ii) the observed re-methylation of the IHg issued from the demethylation.

Hg species isotopic fractionation along the incubation experiments.

No significant MMHg MIF ($\Delta^{199}Hg_{MMHg}$) could be measured in any of the dark controls or the incubation carried out at 3.5 m depth at HU, for which the MMHg degradation was never significant. In the subsurface incubations, the increase in $\Delta^{199}Hg_{MMHg}$ mirrored the decrease in MMHg concentrations as expected and went from 0 to 2.80 ± 0.26 ‰, 5.50 ± 0.67 ‰ and 6.06 ± 0.25 ‰ after 36 h for HU, UU and BC, respectively (Figure 2). The corresponding MDF ($\delta^{202}Hg_{MMHg}$) increased to 0.2 ± 0.1 ‰, 0.7 ± 0.2 ‰ and 0.4 ± 0.1 ‰, leading to an average $\Delta^{199}Hg/\delta^{202}Hg$ of 7.5 ± 0.7 (1 SE, York regression, Figure SI-5), which is higher than the previous reported slope (2.4 ± 0.1, 1 SE).[37,39] However, the variability in the data is large and may originate from other reactions that MMHg undergo besides photodegradation but also from analytical uncertainties.[57] For example, the $\delta^{202}Hg_{MMHg}$ decreased following the re-methylation of the produced IHg in UU waters, consistent with previous observations that lighter Hg isotopes are preferentially taken up and methylated.[68,69]

On the contrary, the MIF of the produced/residual IHg ($\Delta^{199}Hg_{IHg}$) decreased from 0 to -9.9 ± 0.2 ‰, -5.7 ± 0.6 ‰ and -8.5 ± 0.6 ‰ after 36 h for HU, UU and BC, respectively with a plateau phase or a slight decrease during the night period for HU and BC but a slight increase for UU. These negative MIF values mirror the positive MMHg MIF values in BC and UU but not in HU where the photoreduction of IHg is the strongest. The photoreduction of IHg has been found to produce a positive MIF on the remaining IHg[39,44] while UV-B photolysis experiments of Hg^0 in the presence of halogens generated a negative MIF in the produced IHg.[70] We thus suggest that a large fraction of the measured IHg in the HU incubations originates from the re-oxidation of Hg^0, the only mechanism shown to produce negative MIF until now and which is likely favored by our closed incubation bottles. The corresponding MDF ($\delta^{202}Hg_{IHg}$) exhibited two different patterns depending on the stations, an increase to 0.8 ± 0.5 ‰ for UU but a decrease for both HU and BC to -0.7 ± 0.1 ‰ and -0.86 ± 0.1 ‰, respectively. The increase in $\delta^{202}Hg_{IHg}$ observed in UU can be explained by the precipitation of HgS as a positive Hg-MDF was evidenced during this reaction[71] and

this is also consistent with the fact that only a small fraction of the degraded MMHg is recovered as IHg in UU as discussed above (Figure SI-6).

MIF signatures and enrichment factors.

The average $\Delta^{199}Hg/\Delta^{201}Hg$ slope of the residual MMHg was 1.31 ± 0.01 (1 SE, York regression, $r^2 = 0.999$, Figure 3) when considering all data. However, the value for the HU waters (1.24 ± 0.03 with 3 mg L^{-1} DOC, 1 SE, York regression) was significantly lower than the ones for BC and UU (1.33 ± 0.02 and 1.34 ± 0.02 with 6 and 16 mg L^{-1} DOC, respectively, both 1 SE and York regression). Overall, our $\Delta^{199}Hg/\Delta^{201}Hg_{MMHg}$ ratios are lower than previous values obtained through lab experiments that used "open" systems where the Hg° produced is continuously removed and matrix consisting in purified DOM extracts. Indeed, Bergquist and Blum[58] originally reported a ratio of 1.36 ± 0.02 (2 SE) while Chandan et al.[43] later found an average ratio of 1.38 ± 0.02 (2 SE) with experiments conducted with three contrasted DOM extracts and low ratios between MMHg and strong OM-thiol ligands (MMHg:S_{red}-DOM ratios of 10^{-2} to 10^{-1}). Our values are actually closer to the range obtained for higher MMHg:S_{red}-DOM ratios (0.2 - 2) by Chandan et al.[43] while our estimated MMHg:S_{red}-DOM ratios range from 10^{-4} to 6.10^{-3} (Table SI-2). While we cannot explain such difference, our experiments with natural waters also indicate that the Hg-MIF signature imprinted by MMHg photodegradation decreases when the MMHg:S_{red}-DOM increases and point to a control by the MMHg bonding environment, i.e. its distribution between strong OM-thiol ligands (S_{red}-DOM) and weaker inorganic ones such as N and O ligands associated to DOM or dissolved Cl^-.[43] On the other hand, the slope for the measured IHg was 1.30 ± 0.03 (1 SE, York regression, $r^2 = 0.985$) , similar to the residual MMHg. The other reactions affecting IHg such as photo-reduction/oxidation therefore did not significantly change its MIF signature in our experiments.

Regarding enrichment factors, all experimental data points felt on the same line (except one in HU) and the average MIF enrichment factor ($\varepsilon_{\Delta 199}$) for MMHg was -4.8 ± 0.3 ‰ (1 SE, $r^2 = 0.95$, York regression, Figure 4) while the average MDF enrichment factor ($\varepsilon_{\delta 202}$) was -7.1 ± 0.9 ‰ (1 SE, $r^2 = 0.7$, York regression). The larger variability associated to the MDF enrichment factor may originate from other reactions that MMHg undergo besides photodegradation but also from analytical uncertainties.[57] The individual MIF enrichment factors thus did not differ among the three stations that presented contrasted DOC concentrations (3 to 16 mg L^{-1}) but consistent low MMHg:S_{red}-DOM ratio. Our average MIF enrichment factor is slightly higher but comparable to the one originally

determined by Bergquist and Blum[39] (-3.33 ‰ for 1 mg L^{-1} DOC) under natural light and about 3 times lower than the average determined by Chandan et al.[43] for low MMHg:S_{red}-DOM ratios (-14.9 ± 1.2 ‰, 2 SE) but artificial light conditions.

Hg species isotopic composition in fish from Lakes Titicaca and Uru Uru: implications for MMHg photodegradation and aquatic cycling.

Fish collected from Lake Titicaca and Uru Uru display a similar weight (44 ± 11 and 49 ± 13 g, respectively, n = 15 and 28, Table SI-3) but different HgT concentrations with higher values in Uru Uru compared to Titicaca (642 ± 392 vs 354 ± 156 ng g^{-1} d.w., respectively) and MMHg accounting overall for 89 ± 10 % of HgT. The $\delta^{202}Hg_{MMHg}$ values ranged from 0.05 to 1.11 ‰ among the two lakes and were slightly higher in Lake Titicaca (0.82 ± 0.06 ‰, 1 SE) than Uru Uru (0.59 ± 0.04 ‰, 1 SE). The $\Delta^{199}Hg_{MMHg}$ values ranged from 1.1 to 5.9 ‰ and were also significantly higher in Lake Titicaca (4.3 ± 0.4 ‰, 1 SE) compared to Uru Uru (1.7 ± 0.1 ‰, 1 SE). Based on these values and our MIF enrichment factor, we calculated that the extent of MMHg photodegradation before its incorporation into biota ranges from 2 to 31 % and averages 26 ± 2 and 10 ± 1 % in Lake Titicaca and Uru Uru, respectively. These estimates of MMHg photodegradation would be about 30 % higher if the "classical" MIF enrichment factor (-3.33 ‰)[39] was used. These averages correspond to respectively 18 and 3 h of exposition to sunlight before MMHg is either incorporated or escapes the photic zone, and thus over 30 h of residence time for MMHg in Lake Titicaca when assuming 11 h light per day. Overall, the higher concentrations of MMHg found in both water and biota from Lake Uru Uru compared to Titicaca[46], and exemplified here with fish, can be explained by both a higher methylation activity in this lake[47,49] and a lower photodegradation within its water column. This latter can be ascribed to a reduced depth penetration of UV light owing to high DOC and SPM concentrations and also probably to a more efficient scavenging of MMHg by SPM resulting in its downward export.

The $\Delta^{199}Hg/\Delta^{201}Hg_{MMHg}$ ratio ranged from 1.14 to 1.47 and averaged 1.31 ± 0.01 (n = 43, 1 SE), typical of freshwater fish,[37,43] but the average ratio was lower in Lake Titicaca than Uru Uru, 1.24 ± 0.01 vs 1.35 ± 0.01 (1 SE), respectively. These ratios are strikingly similar to the ones determined experimentally for the HU and UU waters indicating that experiments conducted with natural waters and low MMHg concentrations lead to similar MIF expression than the ones recorded in fish from each lake. Assuming that the MIF expression of MMHg during photodegradation is controlled by the MMHg:Sred ratio, it implies that the distribution of MMHg among ligands in

incubations is similar to the ambient one, even if the concentrations of added MMHg are higher than the ambient ones. The lower $\Delta^{199}Hg/\Delta^{201}Hg_{MMHg}$ ratio measured in fish from the oligo-mesotrophic Lake Titicaca thus seems to reflect an overall higher MMHg:S_{red}-DOM ratio in the upper part of its water column compared to the eutrophic Lake Uru Uru. Considering that their demethylation rate constants were similar to the ones obtained from the incubations with enriched isotopes at close to ambient concentrations, it can be eventually concluded that these incubations mimic MMHg *in situ* photodegradation better than laboratory experiments performed with purified DOM extracts as the sole matrix, which relevance was previously questionned.[43]

Finally, our results confirm that the MIF extent and signature of MMHg in fish record both the extent of demethylation and the MMHg bonding environment during its photodegradation.[43] However, given the importance of enrichment factors to infer the extent of MMHg photodegradation in surface waters and considering the remaining uncertainties regarding the influence of water chemistry on MMHg photodegradation and associated isotopic fractionation, there is still clearly a need to conduct a systematic assessment of enrichment factors with contrasted natural waters. More (in situ) incubations should be performed at low MMHg:S_{red}-DOM ratios to obtain representative MIF enrichment factor(s) and decipher the combined effects of DOM as well as inorganic ions concentrations and composition on the expression of MIF. This will further improve our ability to reconstruct the MMHg cycling and controlling factors using biota archives.

Acknowledgments.

This work is a contribution to LA PACHAMAMA (ANR CESA program, N° ANR-13-CESA-0015-01) and ECCO CYTRIX COMIBOL projects. Sylvain Bérail, Erwan Amice and Alexis Groleau are greatly acknowledged for analytical and technical support.

REFERENCES

(1) Streets, D. G.; Devane, M. K.; Lu, Z.; Bond, T. C.; Sunderland, E. M.; Jacob, D. J. All-Time Releases of Mercury to the Atmosphere from Human Activities. *Environ. Sci. Technol.* **2011**, *45* (24), 10485–10491.

(2) Le Faucheur, S.; Campbell, P. G. C.; Fortin, C.; Slaveykova, V. I. Interactions between Mercury and Phytoplankton: Speciation, Bioavailability, and Internal Handling: Mercury-Phytoplankton Interactions. *Environmental Toxicology and Chemistry* **2014**, *33* (6), 1211–1224.

(3) Lavoie, R. A.; Jardine, T. D.; Chumchal, M. M.; Kidd, K. A.; Campbell, L. M. Biomagnification of Mercury in Aquatic Food Webs: A Worldwide Meta-Analysis. *Environ. Sci. Technol.* **2013**, *47* (23), 13385–13394.

(4) Parks, J. M.; Johs, A.; Podar, M.; Bridou, R.; Hurt, R. A.; Smith, S. D.; Tomanicek, S. J.; Qian, Y.; Brown, S. D.; Brandt, C. C.; Palumbo, A. V.; Smith, J. C.; Wall, J. D.; Elias, D. A.; Liang, L. The Genetic Basis for Bacterial Mercury Methylation. *Science* **2013**, *339* (6125), 1332–1335.

(5) Podar, M.; Gilmour, C. C.; Brandt, C. C.; Soren, A.; Brown, S. D.; Crable, B. R.; Palumbo, A. V.; Somenahally, A. C.; Elias, D. A. Global Prevalence and Distribution of Genes and Microorganisms Involved in Mercury Methylation. *Sci. Adv.* **2015**, *1* (9), e1500675–e1500675.

(6) Guedron, S.; Grimaldi, M.; Grimaldi, C.; Cossa, D.; Tisserand, D.; Charlet, L. Amazonian Former Gold Mined Soils as a Source of Methylmercury: Evidence from a Small Scale Watershed in French Guiana. *Water Research* **2011**, *45* (8), 2659–2669.

(7) Eckley, C. S.; Hintelmann, H. Determination of Mercury Methylation Potentials in the Water Column of Lakes across Canada. *Sci. Total Environ.* **2006**, *368* (1), 111–125.

(8) Soerensen, A. L.; Schartup, A. T.; Skrobonja, A.; Bouchet, S.; Amouroux, D.; Liem-Nguyen, V.; Björn, E. Deciphering the Role of Water Column Redoxclines on Methylmercury Cycling Using Speciation Modeling and Observations From the Baltic Sea. *Global Biogeochem. Cycles* **2018**, *32* (10), 1498–1513.

(9) Ortiz, V. L.; Mason, R. P.; Evan Ward, J. An Examination of the Factors Influencing Mercury and Methylmercury Particulate Distributions, Methylation and Demethylation Rates in Laboratory-Generated Marine Snow. *Marine Chemistry* **2015**, *177*, 753–762.

(10) Gascón Díez, E.; Loizeau, J.-L.; Cosio, C.; Bouchet, S.; Adatte, T.; Amouroux, D.; Bravo, A. G. Role of Settling Particles on Mercury Methylation in the Oxic Water Column of Freshwater Systems. *Environ. Sci. Technol.* **2016**, *50* (21), 11672–11679.

(11) Barkay, T.; Miller, S. M.; Summers, A. O. Bacterial Mercury Resistance from Atoms to Ecosystems. *FEMS Microbiol Rev* **2003**, *27* (2–3), 355–384.

(12) Poulain, A. J.; Amyot, M.; Findlay, D.; Telor, S.; Barkay, T.; Hintelmann, H. Biological and Photochemical Production of Dissolved Gaseous Mercury in a Boreal Lake. *Limnol. Oceanogr.* **2004**, *49* (6), 2265–2275.

(13) Wiatrowski, H. A.; Ward, P. M.; Barkay, T. Novel Reduction of Mercury(II) by Mercury-Sensitive Dissimilatory Metal Reducing Bacteria. *Environ. Sci. Technol.* **2006**, *40* (21), 6690–6696.

(14) Hines, M. E.; Faganeli, J.; Adatto, I.; Horvat, M. Microbial Mercury Transformations in Marine, Estuarine and Freshwater Sediment Downstream of the Idrija Mercury Mine, Slovenia. *Applied Geochemistry* **2006**, *21* (11), 1924–1939.

(15) Charlet, L.; Bosbach, D.; Peretyashko, T. Natural Attenuation of TCE, As, Hg Linked to the Heterogeneous Oxidation of Fe(II): An AFM Study. *Chem. Geol.* **2002**, *190* (1–4), 303–319.

(16) O'Loughlin, E. J.; Kelly, S. D.; Kemner, K. M.; Csencsits, R.; Cook, R. E. Reduction of AgI, AuIII, CuII, and Hg II by FeII/FeIII Hydroxysulfate Green Rust. *Chemosphere* **2003**, *53* (5), 437–446.

(17) Allard, B.; Arsenie, I. Abiotic Reduction of Mercury by Humic Substances in Aquatic System - An Important Process for the Mercury Cycle. *Water, Air, and Soil Pollution* **1991**, *56* (SPEC. VOL.), 457–464.

(18) Gu, B.; Bian, Y.; Miller, C. L.; Dong, W.; Jiang, X.; Liang, L. Mercury Reduction and Complexation by Natural Organic Matter in Anoxic Environments. *Proc. Natl. Acad. Sci. USA* **2011**, *108*, 1479–1483.

(19) Jiang, T.; Kaal, J.; Liu, J.; Liang, J.; Zhang, Y.; Wang, D. Linking the Electron Donation Capacity to the Molecular Composition of Soil Dissolved Organic Matter from the Three Gorges Reservoir Areas, China. *Journal of Environmental Sciences* **2020**, *90*, 146–156.

(20) Sellers, P.; Kelly, C. A.; Rudd, J. W. M.; MacHutchon, A. R. Photodegradation of Methylmercury in Lakes. *Nature* **1996**, *380* (6576), 694–697.

(21) Amyot, M.; Lean, D.; Mierle, G. Photochemical Formation of Volatile Mercury in High Arctic Lakes. *Environmental Toxicology and Chemistry* **1997**, *16* (10), 2054–2063.

(22) Black, F. J.; Poulin, B. A.; Flegal, A. R. Factors Controlling the Abiotic Photo-Degradation of Monomethylmercury in Surface Waters. *Geochimica et Cosmochimica Acta* **2012**, *84*, 492–507.

(23) Hammerschmidt, C. R.; Fitzgerald, W. F. Photodecomposition of Methylmercury in an Arctic Alaskan Lake. *Environ. Sci. Technol.* **2006**, *40* (4), 1212–1216.

(24) Sun, R.; Wang, D.; Zhang, Y.; Mao, W.; Zhang, T.; Ma, M.; Zhang, C. Photo-Degradation of Monomethylmercury in the Presence of Chloride Ion. *Chemosphere* **2013**, *91* (11), 1471–1476.
(25) Lehnherr, I.; St. Louis, V. L. Importance of Ultraviolet Radiation in the Photodemethylation of Methylmercury in Freshwater Ecosystems. *Environ. Sci. Technol.* **2009**, *43* (15), 5692–5698.
(26) O'Driscoll, N. J.; Lean, D. R. S.; Loseto, L. L.; Carignan, R.; Siciliano, S. D. Effect of Dissolved Organic Carbon on the Photoproduction of Dissolved Gaseous Mercury in Lakes: Potential Impacts of Forestry. *Environmental Science and Technology* **2004**, *38* (9), 2664–2672.
(27) Garcia, E.; Amyot, M.; Ariya, P. A. Relationship between DOC Photochemistry and Mercury Redox Transformations in Temperate Lakes and Wetlands. *Geochimica et Cosmochimica Acta* **2005**, *69* (8), 1917–1924.
(28) Klapstein, S. J.; O'Driscoll, N. J. Methylmercury Biogeochemistry in Freshwater Ecosystems: A Review Focusing on DOM and Photodemethylation. *Bulletin of Environmental Contamination and Toxicology* **2018**, *100* (1), 14–25.
(29) Yang, J.; Kim, J.; Soerensen, A. L.; Lee, W.; Han, S. The Role of Fluorescent Dissolved Organic Matter on Mercury Photoreduction Rates: A Case Study of Three Temperate Lakes. *Geochimica et Cosmochimica Acta* **2020**.
(30) Xiao, Z. F.; Strömberg, D.; Lindqvist, O. Influence of Humic Substances on Photolysis of Divalent Mercury in Aqueous Solution. In *Mercury as a Global Pollutant: Proceedings of the Third International Conference held in Whistler, British Columbia, July 10–14, 1994*; Porcella, D. B., Huckabee, J. W., Wheatley, B., Eds.; Springer Netherlands: Dordrecht, 1995; pp 789–798.
(31) Zhang, T.; Hsu-Kim, H. Photolytic Degradation of Methylmercury Enhanced by Binding to Natural Organic Ligands. *Nature Geoscience* **2010**, *3* (7), 473–476.
(32) Klapstein, S. J.; Ziegler, S. E.; O'Driscoll, N. J. Methylmercury Photodemethylation Is Inhibited in Lakes with High Dissolved Organic Matter. *Environmental Pollution* **2018**, *232*, 392–401.
(33) Jeremiason, J. D.; Portner, J. C.; Aiken, G. R.; Hiranaka, A. J.; Dvorak, M. T.; Tran, K. T.; Latch, D. E. Photoreduction of Hg(II) and Photodemethylation of Methylmercury: The Key Role of Thiol Sites on Dissolved Organic Matter. *Environ. Sci.: Processes Impacts* **2015**, *17* (11), 1892–1903.
(34) Fernández-Gómez, C.; Drott, A.; Björn, E.; Díez, S.; Bayona, J. M.; Tesfalidet, S.; Lindfors, A.; Skyllberg, U. Towards Universal Wavelength-Specific Photodegradation Rate Constants for Methyl Mercury in Humic Waters, Exemplified by a Boreal Lake-Wetland Gradient. *Environ. Sci. Technol.* **2013**, *47* (12), 6279–6287.
(35) Qian, Y.; Yin, X.; Lin, H.; Rao, B.; Brooks, S. C.; Liang, L.; Gu, B. Why Dissolved Organic Matter Enhances Photodegradation of Methylmercury. *Environmental Science & Technology Letters* **2014**, *1* (10), 426–431.
(36) Zhang, X.; Li, Y.; Feng, G.; Tai, C.; Yin, Y.; Cai, Y.; Liu, J. Probing the DOM-Mediated Photodegradation of Methylmercury by Using Organic Ligands with Different Molecular Structures as the DOM Model. *Water Research* **2018**, *138*, 264–271.
(37) Blum, J. D.; Sherman, L. S.; Johnson, M. W. Mercury Isotopes in Earth and Environmental Sciences. *Annu. Rev. Earth. Pl. Sc.* **2014**, *42* (1), 249–269.
(38) Blum, J. D.; Popp, B. N.; Drazen, J. C.; Anela Choy, C.; Johnson, M. W. Methylmercury Production below the Mixed Layer in the North Pacific Ocean. *Nature Geosci* **2013**, *6* (10), 879–884.
(39) Bergquist, B. A.; Blum, J. D. Mass-Dependent and -Independent Fractionation of Hg Isotopes by Photoreduction in Aquatic Systems. *Science* **2007**, *318* (5849), 417–420.
(40) Malinovsky, D.; Latruwe, K.; Moens, L.; Vanhaecke, F. Experimental Study of Mass-Independence of Hg Isotope Fractionation during Photodecomposition of Dissolved Methylmercury. *Journal of Analytical Atomic Spectrometry* **2010**, *25* (7), 950.
(41) Zheng, W.; Hintelmann, H. Mercury Isotope Fractionation during Photoreduction in Natural Water Is Controlled by Its Hg/DOC Ratio. *Geochimica et Cosmochimica Acta* **2009**, *73* (22), 6704–6715.
(42) Zheng, W.; Hintelmann, H. Isotope Fractionation of Mercury during Its Photochemical Reduction by Low-Molecular-Weight Organic Compounds. *J. Phys. Chem. A* **2010**, *114* (12), 4246–4253.
(43) Chandan, P.; Ghosh, S.; Bergquist, B. A. Mercury Isotope Fractionation during Aqueous Photo-Reduction of Monomethylmercury in the Presence of Dissolved Organic Matter. *Environmental Science & Technology* **2014**, 141117013917004.
(44) Rose, C. H.; Ghosh, S.; Blum, J. D.; Bergquist, B. A. Effects of Ultraviolet Radiation on Mercury Isotope Fractionation during Photo-Reduction for Inorganic and Organic Mercury Species. *Chemical Geology* **2015**, *405*, 102–111.
(45) Achá, D.; Guédron, S.; Amouroux, D.; Point, D.; Lazzaro, X.; Fernandez, P. E.; Sarret, G. Algal Bloom Exacerbates Hydrogen Sulfide and Methylmercury Contamination in the Emblematic High-Altitude Lake Titicaca. *Geosciences* **2018**, *8* (12), 438.
(46) Guédron, S.; Point, D.; Acha, D.; Bouchet, S.; Baya, P. A.; Tessier, E.; Monperrus, M.; Molina, C. I.; Groleau, A.; Chauvaud, L.; Thebault, J.; Amice, E.; Alanoca, L.; Duwig, C.; Uzu, G.; Lazarro, X.; Bertrand, A.; Bertrand, S.;

Barbraud, C.; Delord, K.; Gibon, F. M.; Ibanez, C.; Flores, M.; Fernandez Saavedra, P.; Ezpinoza, M. E.; Heredia, C.; Rocha, F.; Zepita, C.; Amouroux, D. Mercury Contamination Level and Speciation Inventory in Lakes Titicaca & Uru-Uru (Bolivia): Current Status and Future Trends. *Environ. Pollut.* **2017**, *231*, 262–270.

(47) Alanoca, L.; Amouroux, D.; Monperrus, M.; Tessier, E.; Goni, M.; Guyoneaud, R.; Acha, D.; Gassie, C.; Audry, S.; Garcia, M. E.; Quintanilla, J.; Point, D. Diurnal Variability and Biogeochemical Reactivity of Mercury Species in an Extreme High-Altitude Lake Ecosystem of the Bolivian Altiplano. *Environ. Sci. Poll. Res.* **2016**, *23* (7), 6919–6933.

(48) Lanza, W. G.; Achá, D.; Point, D.; Masbou, J.; Alanoca, L.; Amouroux, D.; Lazzaro, X. Association of a Specific Algal Group with Methylmercury Accumulation in Periphyton of a Tropical High-Altitude Andean Lake. *Arch. Environ. Con. Tox.* **2017**, *72* (1), 1–10.

(49) Bouchet, S.; Goñi-Urriza, M.; Monperrus, M.; Guyoneaud, R.; Fernandez, P.; Heredia, C.; Tessier, E.; Gassie, C.; Point, D.; Guédron, S.; Achá, D.; Amouroux, D. Linking Microbial Activities and Low-Molecular-Weight Thiols to Hg Methylation in Biofilms and Periphyton from High-Altitude Tropical Lakes in the Bolivian Altiplano. *Environmental Science & Technology* **2018**, *52* (17), 9758–9767.

(50) Guédron, S.; Audry, S.; Acha, D.; Bouchet, S.; Point, D.; Condom, T.; Heredia, C.; Campillo, S.; Baya, P. A.; Groleau, A.; Amice, E.; Amouroux, D. Diagenetic Production, Accumulation and Sediment-Water Exchanges of Methylmercury in Contrasted Sediment Facies of Lake Titicaca (Bolivia). *Science of The Total Environment* **2020**, *723*, 138088.

(51) Morrow, J. H.; Booth, C. R.; Lind, R. N.; Hooker, S. R. The Compact Optical Profiling System (C-OPS). In *J.H. Morrow, S.B. Hooker, C.R. Booth, G. Bernhard, R.N. Lind, and J.W. Brown, Advances in Measuring the Apparent Optical Properties (AOPs) of Optically Complex Waters*; NASA Tech. Memo; NASA Goddard Space Flight Center, Greenbelt, Maryland, 2010; Vol. 2010–215856, pp 42–50.

(52) Northcote, T. G. Ecological Interactions among an Orestiid (Pisces: Cyprinodontidae) Species Flock in the Littoral Zone of Lake Titicaca. In *Advances in Ecological Research*; Ancient Lakes: Biodiversity, Ecology and Evolution; Academic Press, 2000; Vol. 31, pp 399–420.

(53) Masbou, J.; Point, D.; Sonke, J. E. Application of a Selective Extraction Method for Methylmercury Compound Specific Stable Isotope Analysis (MeHg-CSIA) in Biological Materials. *J. Anal. At. Spectrom.* **2013**, *28* (10), 1620–1628.

(54) Bouchet, S.; Tessier, E.; Monperrus, M.; Bridou, R.; Clavier, J.; Thouzeau, G.; Amouroux, D. Measurements of Gaseous Mercury Exchanges at the Sediment-Water, Water-Atmosphere and Sediment-Atmosphere Interfaces of a Tidal Environment (Arcachon Bay, France). *J. Environ. Monitor* **2011**, *13* (5), 1351–1359.

(55) Rodriguez-Gonzalez, P.; Bouchet, S.; Monperrus, M.; Tessier, E.; Amouroux, D. In Situ Experiments for Element Species-Specific Environmental Reactivity of Tin and Mercury Compounds Using Isotopic Tracers and Multiple Linear Regression. *Environ. Sci. Poll. Res.* **2013**, *20* (3), 1269–1280.

(56) Monperrus, M.; Tessier, E.; Veschambre, S.; Amouroux, D.; Donard, O. Yan. *Anal. Bioanal. Chem.* **2005**, *381* (4), 854–862.

(57) Bouchet, S.; Bérail, S.; Amouroux, D. Hg Compound-Specific Isotope Analysis at Ultratrace Levels Using an on Line Gas Chromatographic Preconcentration and Separation Strategy Coupled to Multicollector-Inductively Coupled Plasma Mass Spectrometry. *Analytical Chemistry* **2018**, *90* (13), 7809–7816.

(58) Blum, J. D.; Bergquist, B. A. Reporting of Variations in the Natural Isotopic Composition of Mercury. *Anal. Bioanal. Chem.* **2007**, *388* (2), 353–359.

(59) Epov, V. N.; Berail, S.; Jimenez-Moreno, M.; Perrot, V.; Pecheyran, C.; Amouroux, D.; Donard, O. F. X. Approach to Measure Isotopic Ratios in Species Using Multicollector-ICPMS Coupled with Chromatography. *Anal. Chem.* **2010**, *82* (13), 5652–5662.

(60) Archundia, D.; Duwig, C.; Spadini, L.; Uzu, G.; Guédron, S.; Morel, M. C.; Cortez, R.; Ramos Ramos, O.; Chincheros, J.; Martins, J. M. F. How Uncontrolled Urban Expansion Increases the Contamination of the Titicaca Lake Basin (El Alto, La Paz, Bolivia). *Water, Air, & Soil Pollution* **2017**, *228* (1).

(61) Tai, C.; Li, Y.; Yin, Y.; Scinto, L. J.; Jiang, G.; Cai, Y. Methylmercury Photodegradation in Surface Water of the Florida Everglades: Importance of Dissolved Organic Matter-Methylmercury Complexation. *Environmental Science & Technology* **2014**, *48* (13), 7333–7340.

(62) Kim, M.-K.; Zoh, K.-D. Effects of Natural Water Constituents on the Photo-Decomposition of Methylmercury and the Role of Hydroxyl Radical. *Science of The Total Environment* **2013**, *449*, 95–101.

(63) Zhang, D.; Yin, Y.; Li, Y.; Cai, Y.; Liu, J. Critical Role of Natural Organic Matter in Photodegradation of Methylmercury in Water: Molecular Weight and Interactive Effects with Other Environmental Factors. *Science of The Total Environment* **2017**, *578*, 535–541.

(64) Girard, C.; Leclerc, M.; Amyot, M. Photodemethylation of Methylmercury in Eastern Canadian Arctic Thaw Pond and Lake Ecosystems. *Environmental Science & Technology* **2016**, *50* (7), 3511–3520.

(65) Guédron, S.; Achá, D.; Bouchet, S.; Point, D.; Tessier, E.; Heredia, C.; Rocha-Lupa, S.; Fernandez-Saavedra, P.; Flores, M.; Bureau, S.; Quino-Lima, I.; Amouroux, D. Accumulation of Methylmercury in the High-Altitude Lake Uru Uru (3686 m a.s.l, Bolivia) Controlled by Sediment Efflux and Photodegradation. *Applied Sciences* **2020**, *10* (21), 7936.

(66) Si, L.; Ariya, P. A. Photochemical Reactions of Divalent Mercury with Thioglycolic Acid: Formation of Mercuric Sulfide Particles. *Chemosphere* **2015**, *119*, 467–472.

(67) Manceau, A.; Lemouchi, C.; Enescu, M.; Gaillot, A.-C.; Lanson, M.; Magnin, V.; Glatzel, P.; Poulin, B. A.; Ryan, J. N.; Aiken, G. R.; Gautier-Luneau, I.; Nagy, K. L. Formation of Mercury Sulfide from Hg(II)–Thiolate Complexes in Natural Organic Matter. *Environ. Sci. Technol.* **2015**, *49* (16), 9787–9796.

(68) Rodríguez-González, P.; Epov, V. N.; Bridou, R.; Tessier, E.; Guyoneaud, R.; Monperrus, M.; Amouroux, D. Species-Specific Stable Isotope Fractionation of Mercury during Hg(II) Methylation by an Anaerobic Bacteria (Desulfobulbus Propionicus) under Dark Conditions. *Environ. Sci. Technol.* **2009**, *43* (24), 9183–9188.

(69) Wang, Y.; Janssen, S. E.; Schaefer, J. K.; Yee, N.; Reinfelder, J. R. Tracing the Uptake of Hg(II) in an Iron-Reducing Bacterium Using Mercury Stable Isotopes. *Environ. Sci. Technol. Lett.* **2020**, *7* (8), 573–578.

(70) Sun, G.; Sommar, J.; Feng, X.; Lin, C.-J.; Ge, M.; Wang, W.; Yin, R.; Fu, X.; Shang, L. Mass-Dependent and -Independent Fractionation of Mercury Isotope during Gas-Phase Oxidation of Elemental Mercury Vapor by Atomic Cl and Br. *Environ. Sci. Technol.* **2016**, *50* (17), 9232–9241.

(71) Smith, R. S.; Wiederhold, J. G.; Kretzschmar, R. Mercury Isotope Fractionation during Precipitation of Metacinnabar (β-HgS) and Montroydite (HgO). *Environ. Sci. Technol.* **2015**, *49* (7), 4325–4334.

Table of content (TOC)/Abstract Art.

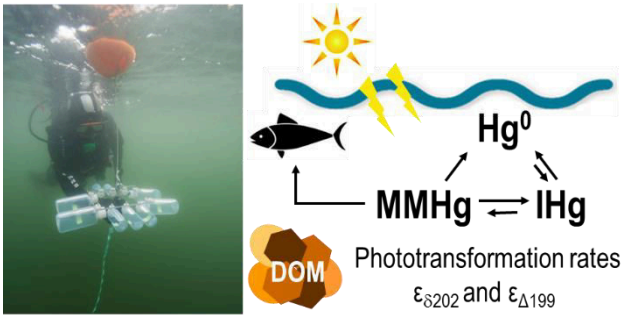

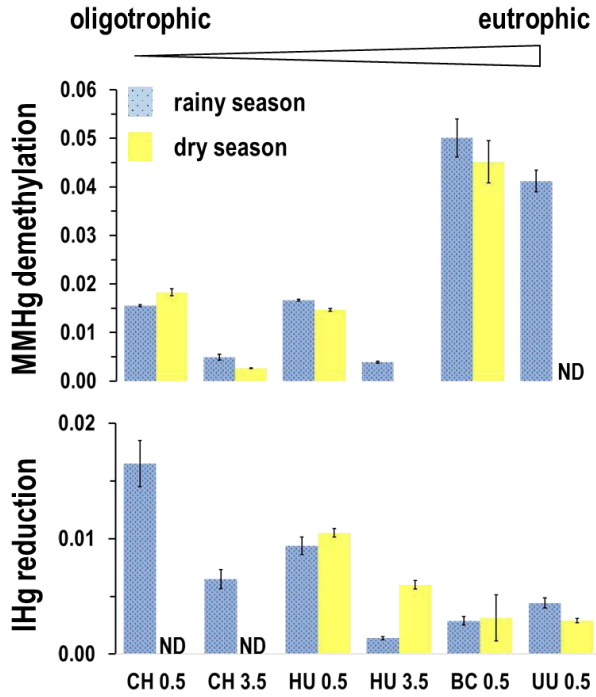

Figure 1: MMHg demethylation and IHg reduction rate constants (in h^{-1}, error bars represent 1 sd of triplicate incubations) determined with isotopically enriched tracers over the 2 seasons and for the various stations and depths (0.5 and/or 3.5 m) investigated.

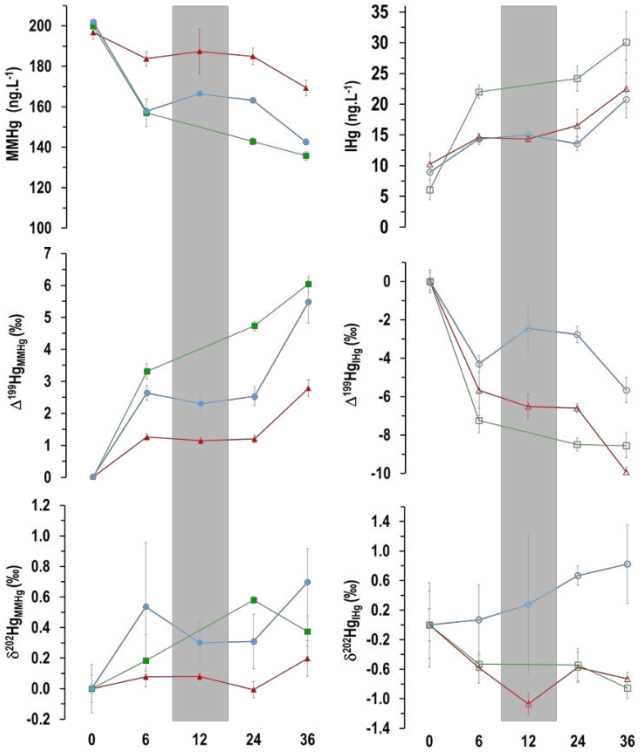

Figure 2: Average concentrations (upper panels), Hg mass independent (middle panels) and mass dependent fractionation (lower panels) of MMHg and IHg along time (x axis in h) in the stable isotope incubations experiments (error bars represent 1 sd of triplicate incubations and shaded areas the night period, red trianges: HU, green squares: BC and blue circles: UU). All isotopic composition data were normalized to t_0 in order to correct for the fractionation that occurred upon addition of MMHg.

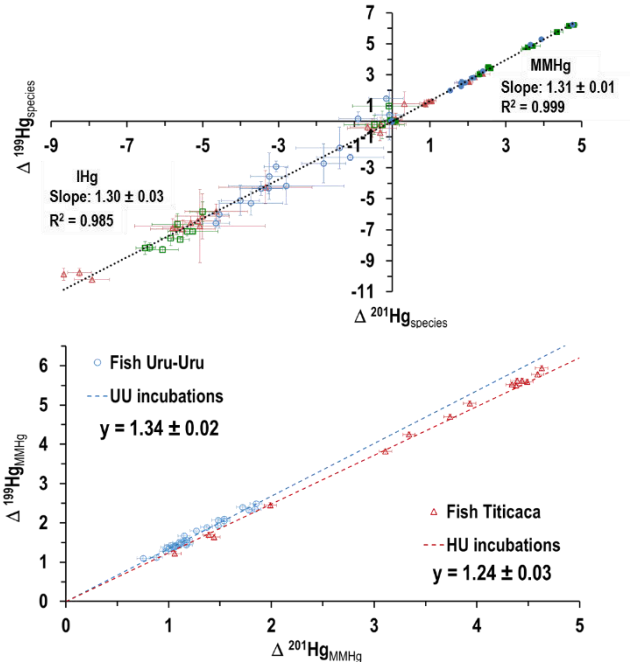

Figure 3: Upper panel: Δ^{199}Hg vs Δ^{201}Hg for MMHg (right part) and IHg (left part) in the incubation experiments (red triangles: HU, green squares: BC and blue circles: UU, each point represents an individual experiment and error bars 1 sd of triplicate measurements). Lower panel: Δ^{199}Hg vs Δ^{201}Hg for MMHg recorded in fish from each lakes superimposed on the regression lines obtained from the incubation experiments.

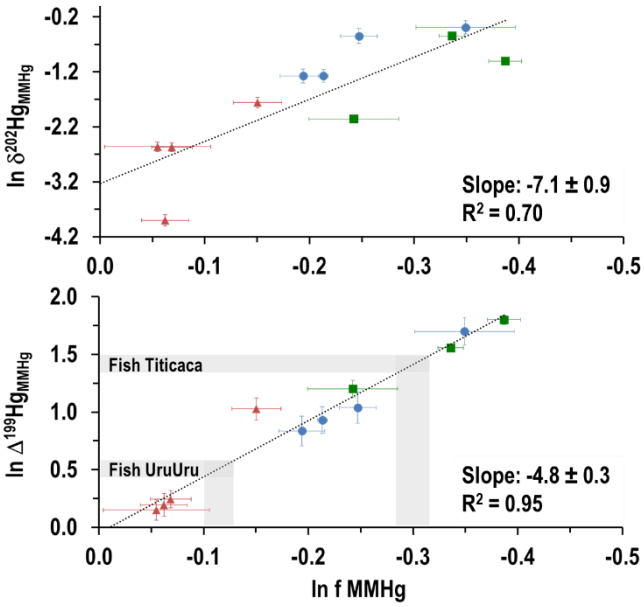

Figure 4: Hg_{MMHg} mass dependent (upper panel) and independent (lower panel) fractionation as a function of demethylation yield along the incubations (error bars represent 1 sd of triplicate incubations, red triangles: HU, green squares: BC and blue circles: UU). Grey bands indicate the $\Delta^{199}Hg_{MMHg}$ values (Compound Specific Isotopic Analysis) recorded in fish from each lake (mean ± 1 SE).